International Journal of Advances in Engineering and Management (IJAEM)
Volume 6, Issue 09 Sep. 2024, pp: 321-339 www.ijaem.net ISSN: 2395-5252

Fin sensitivity studies to Dampen Yaw Motion Response in Shallow Water

Dick, Ibitoru. F [(a)], Orji, Charles. U [(ab)], Ibekwe, A. U [(b)], Douglas, Ibiba. E[(ab)]

[(a)] *Department of Marine Engineering, Faculty of Engineering, Rivers State University, Nkpolu-Oroworukwo, Port Harcourt, Nigeria*

[(b)] *NNPC/SPDC-JV Centre of Excellence in Marine and Offshore Engineering, Rivers State University, Port Harcourt, Nigeria*

Date of Submission: 10-09-2024 Date of Acceptance: 20-09-2024

ABSTRACT

This work is predicated upon the need to determine optimum fin size, angle of attachment and sea state that would guarantee practicably all-encompassing safety for a moored Mystery FPSO against problematic shallow water-induced yaw response amplitude arising from wave drift forces. Three pairs of fin sizes were thus parametrically selected of widths 4.23mm, 8.46mm and 12.69mm with respective aspect ratios 0.0313, 0.0627 and 0.094 at 0^O, 15^O and 30^O angles of attachments to the Mystery FPSO hull. Results from a developed matrix for numerical investigations involving 72 runs, 24 runs for each fin size, showed that for all the considered fin angles for fin size 4.23mm, the oblique sea direction 30^O presented the best all-positive percentage reductions in yaw motion response amplitude with an average of 7.6%. Again, for all the considered fin angles for fin size 8.46mm, the beam sea direction, 90^O, presented the best all-positive percentage reductions in yaw motion response amplitude with an average of 10.6%. In the 12.69mm fin size category, it was shown that the 30^O oblique sea condition produced the all-positive percentage reductions in yaw motion response amplitude with an average of 20.3%. However, a more interesting result was obtained across all tested sea conditions for fin size 8.46mm at 0^O point of attachment to the FPSO hull. Only at this point of attachment in all sea directions were all percentage reductions in yaw motion response amplitudes found all-positive with an average percentage reduction of 17.8%. This is more practical as moored FPSOs are designed to face site-specific sea conditions, whether in the pure or interacting forms, for operational survivability and not for impact forces from a single sea state. This preferentially puts fin size 8.46mm at 0^O point of attachment, despite having lower average percentage reduction in yaw motion response amplitude relative to fin size 12.69mm, to be presenting the best operational safety net against wave drift forces in the investigated shallow water depth for the FPSO in all tested sea states. Validation experiment showed congruence between numerical and experimental results within 10 % root-mean-square-error. Thus, it is concluded that the obtained 17.8% reduction in yaw response amplitude is achievable with an optimum fin size of 8.46mm at fin angle 0^O across all investigated sea conditions within 90% accuracy level to guarantee additional operational safety.

Keywords: Optimum Fin Selection, Shallow Water, Vertical Orientation, Wave Drift Force, Yaw Response Amplitude Reduction.

I. INTRODUCTION

Motion studies for floating ocean structures whether surface-piercing or deeply submerged, moored or with forward speed are usually conducted to verify capacity in terms of strength and performance factored-in in their designed. These analyses are usually required by regulation during the design stages of these structures where tests are carried out using models of the prototype in a towing tank or simulation of the prototype/model in proven hydrodynamics software as full-scale analysis is seen too expensive to conduct. Until satisfactory results are obtained, construction of designed structures is not done. Acceptable performance against vessel responses to hydrodynamic excitation forces is a necessity for operability particularly for moored structures that must maintain position for effective productive operations. If hull optimization solution cannot guarantee acceptable performance for underperforming designs, then, motion damping mechanism becomes the alternative.

As postulated by (Smith & Thomas, 1990), the need to reduce ship motions spanned across economics and readiness and not limited only to the comfort of ship's crew and so should be examined properly. They held that among the six degrees of freedom of vessel motion response, only heave, roll and pitch exhibit resonance while the horizontal motions such as surge, sway and yaw do not exhibit resonance as these do not possess restoring force. Consequently, they are categorized under maneuvering where directional stability of ships is a major concern. Hence, heave, pitch and roll become the most likely motion reduction problem, they stated.

Contrasting the above, Johannes (1980) had earlier postulated that yaw motion among the horizontal motions becomes more problematic and requires reduction when vessel is excited by second order wave drift forces particularly at the horizontal water plane. This contrast is not unexpected owing to the dynamics of research as new technologies evolve arising from better understanding of the physics of water mechanics. More recently, corroborated Johannes' earlier position where the authors discovered that the horizontal component of the order 2 mean and low frequency wave force, also known as wave drift force, can impact a steady slow drift motion on floating vessels in the general direction of wave propagation, if not restrained. According to their findings, this becomes critically most severe in shallow waters where the horizontal component of the orbital velocity transcends the seabed with minimal degradation thus, producing a damaging effect on the mooring equipment and other attached hull appurtenances and resulting vessel instability.

Several works have been done affirming the severity of shallow water-induced problematic yaw response amplitude arising from wave drift forces. A few among these are the works of (Lingzhi et al., 2015) which considered 3-D potential flow in both time and frequency domains experimentally and numerically. The authors held that low frequency motions were more sensitive to shallow water effects than wave frequency motions for moored barge structure. Again, Sanchez et al., (2018) detected large slow yaw rotation via experimental studies against regular and irregular wave conditions on a turret-moored FPSO in a wave basin. They further identified dangerous regular wave periods that could trigger large yaw rotation. Simulation on a time domain basis with changing turret position relative to FPSO's Centre of gravity, also revealed that large yaw motion could quickly be provoked with the turret closest to the Centre of gravity of the FPSO. Other works in this category which supports yaw motion response reduction includes works by Wichers, 2013, Molin and Fauveau, (1984), Yang et al., (2002), Li et al., (2003), Naciri et al., (2004), Wim and Ivo (2008), Pinkster, (2009), Yan et al., (2010), etc.

Motion dampening mechanisms have been rigorously reviewed by (Smith & Thomas, 1990). Rajesh et al., (2016) and Smith & Thomas, (1990) had reported on the successful application of fins for extensive control of pitch and roll motions and of course, other interacting motion forms such as sway, surge, and yaw on a lighter note for vessels with forward speed. In these applications, the fins are either horizontal or slightly tilted from the horizontal waterplane and deeply submerged. Again, Dynamic Positioning (DP) system have also been reported of possessing excellent capability for motion control of moored structures in all six degrees of freedom of motions. It has been noted that the application of dynamic positioning (DP) system can even control vessel horizontal motions to avoid instability caused by inappropriate positioning of a turret system in a moored FPSO (Greco, etal, 2015). However, the difficult challenges when operating in shallow waters leading to complex control architecture and associated cost as alluded to, by (IMCA, 2016) in their review work titled "DP Position loss risks in shallow waters" calls for an alternative engineering solution.

Engineering solutions when not cost effective are not optimal therefore, the main driver for this current research is to provide a simple and seemingly cost-effective solution by the application of surface-piercing and vertically oriented rectangular passive fin on a moored FPSO at the fore and aft peaks for the reduction of the problematic shallow water-induced yaw response amplitude arising from wave drift forces. In the procedure applied, use is made of the recommendations from Mc Taggart, (2004) for the fin to be surface piercing to capture both radiative and diffraction forces for large volume bodies. This is, indeed, a deviation from reported profiles and positions of fins that are aero-foil in shape, deeply submerged, purely horizontal or at some angle away from the horizontal waterplane and streamlined with the fluid flow. Selection of fin parameters is guided by the recommendation from Rajesh et al., (2016) and Wendi et al., (2019). Here, the intent is to investigate the extensive applicability of the rules for parameter selection of bilge keels to fins and to leverage on the passive viscous damping property of fins at low speed. The investigation is limited to the shallow water regular wave of the Gulf of Guinea incorporating both experimental and numerical solution procedures. The investigation water depth is 144m. This limit is set by the capability of the validation towing tank facility. Analysis considered Beam Seas (90^o), Head Sea (180^o) and two Oblique Sea conditions (30^o and 60^o) capable of testing for motion response in all six degrees of freedom condition but with particular interest in Yaw motion response (Jaime & Longbin, 2017).

Thus, the following objectives will help achieve the aim.

i. To parametrically select three pairs of rectangular fins for sensitivity studies
ii. To develop two numerical models of Mystery FPSO vessel, one without fins (Bare Hull) and the other with each of the selected fins attached to the hull, using proven hydrodynamic Software, MAXSURF & ANSYS AQWA/HydroD and subjecting them to candidate sea states for motion studies.
iii. To analyze and compare yaw time series response signatures resulting from step 2 above to establish possibility of motion response damping due to the attached fin.
iv. To analyze Fourier-transformed yaw time series response data obtained for the Bare hull and fin-attached FPSO models to determine critical frequency band for peak motion response, the extent of damping achieved through statistical analysis and to optimally select the best fin size.
v. To carry out analysis using results from experimental studies of the FPSO model under the same numerical investigation conditions in the towing tank facility of NNPC/SPDC-JV Centre of excellence in Marine and offshore engineering of the Rivers State University, Port Harcourt, in order to validate the numerical results.

II. MATERIALS AND METHODS

2.1: Materials

2.1.1: Metocean Data

For the hydrodynamic analysis of any moored Offshore structure, site specific conditions are usually applied to factor-in representative hydrodynamic influence in the analysis. Hence, Table 1 shows 100-year return period wave data for the Gulf of Guinea used for both analyses.

Table 1: Joint Criteria for Extreme Dominated Swell Wave for 100yr Return

Parameter	100 Years
Significant wave Height (m)	3.45
Peak period (s)	17

(Source: Ekwere et al., (2021))

2.1.2: Test Sea States.

Sea states critical to various degrees of freedom of motions for test follows as provided by (Jaime & Longbin, 2017).

- Head sea condition (180^0) for surge, heave, and pitch motion RAOs
- Beam sea incident wave condition (90^o) for roll, sway, and yaw motion RAOs
- Oblique sea condition (135^o) for all motions in the 6dof such as surge, sway, heave, roll, pitch, and yaw RAOs

2.1.3: Vertical Rectangular fin parameters

The following dimensions, locations, and orientation for three (3) pairs of fins as shown in Table 2 were chosen for both analyses. The selection of the fin parameters was guided by the recommendation of (Rajesh et al., 2016; McTaggart, 2004 and Wendi et al., 2019) to capture desired results. Figure 1 shows the models of the candidate fin sizes and profile used for the experimental study.

Table 2: Vertical Fin Dimensions for FPSO

	Width & Aspect Ratio		Thickness		Depth		
Size	Prototype	Model	Prototype	Model	Prototype	Model	Shape/Orientation
1	0.51m	4.23mm	10mm	4mm	Keel to w.deck	Keel to w.deck	Rectangular/Vertical
	A/R	0.0313					
2	1.015m	8.46mm	10mm	4mm	Keel to w.deck	Keel to w.deck	Rectangular/Vertical
	A/R	0.0627					
3	1.523m	12.69mm	10mm	4mm	Keel to w.deck	Keel to w.deck	Rectangular/Vertical
	A/R	0.0940					

(Source: (Rajesh et al., 2016; McTaggart, 2004 and Wendi et al., 2019)

International Journal of Advances in Engineering and Management (IJAEM)
Volume 6, Issue 09 Sep. 2024, pp: 321-339 www.ijaem.net ISSN: 2395-5252

2.1.4: Fin Profile

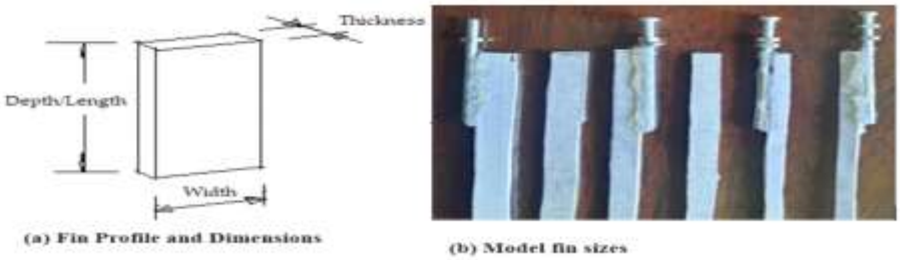

Figure 1: Fin Dimensions, Orientation and Profile

2.1.5: Plan view of FPSO hull showing points of attachment of fin.

The angular orientation of the fins, towards portside at the fore and towards starboard at the aft peaks as seen in Figure 2 is to ensure effectiveness of the fin.

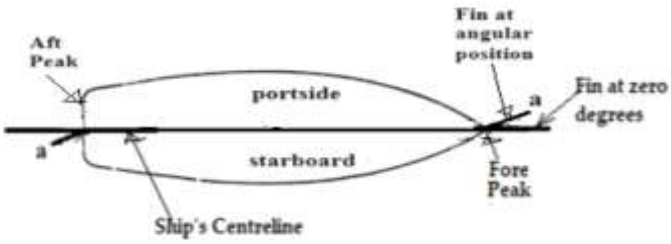

Figure 2: Plan view of FPSO hull showing points of attachment of fins.

2.1.6: FPSO Wooden Model

FPSO wooden model used for the experimental investigation is shown in Figure 3 while the principal parameters are shown in Table 3.

Figure 3: Mystery FPSO Wooden Experimental Model.

2.1.7: Mystery FPSO Vessel Parameters

Principal parameters of the FPSO prototype and Model used for the investigations are shown in Table 3 on a scale of 1:120

International Journal of Advances in Engineering and Management (IJAEM)
Volume 6, Issue 09 Sep. 2024, pp: 321-339 www.ijaem.net ISSN: 2395-5252

Table 3: Mystery FPSO Prototype and Scaled Model Particulars

S/N	Particulars	Prototype	Model
1	Length Overall, LOA (m)	183	1.525
2	Length Between Perpendiculars, LBP (m)	171	1.425
3	Depth, D (m)	16.2	0.135
4	Maximum load draft, d (m)	9.0	0.075
5	Beam, B (m)	25.2	0.21
6	Freeboard at Maximum draft (m)	7.2	0.06
7	50% load draft (m)	4.49	0.0374
8	Longitudinal Centre of Floatation @ maximum load draft (m)	77.86	0.6488
9	Longitudinal Centre of Floatation @ 50% load draft (m)	78.84	0.657
	Block Coefficient	0.83	0.83
10	Displacement(t)	32,994.4671	0.0186283125
	Mass/Weight(kg)	323,675.72251	0.1827437456
11	Wave (m)	3.45	0.02875
12	Period (Sec)	17	1.283 (T. tank limit)

2.1.8: NNPC/SPDC-JV COE Hydrodynamic Towing tank, Rivers State University.

Figure 4 shows the model under investigation against Oblique and Head Seas in the NNPC/SPDC-JV COE Hydrodynamic Towing tank. The tank is 60m long, 2m wide and 2m deep. Operational water depth tapers from 1.5m at the wave maker end to 1.8m at the beach end. The carriage has a maximum tow speed of 3m/s. The tank simulates regular waves in shallow water depth and so, appropriate for this study.

(a) Wooden FPSO Model at Oblique sea condition during experimental studies

(b) Wooden FPSO Model at Head sea condition during experimental studies

Figure 4: Mystery FPSO wooden model at the NNPC/SPDC-JV COE Hydrodynamic Towing tank facility, Rivers State University, Port Harcourt, Nigeria.

2.1.9: Numerical Software deployed

(i) ANSYS AQWA/HydroD version 19.1 This is a proven hydrodynamic software with capabilities for investigating vessel motion responses in regular and irregular wave scenarios. It's based on Potential flow approximations.

(ii) BENTLEYMARXSURF ENTERPRISE 8i version 11.1.

This software has capabilities for model generation and can perform stability and motion analyses. Required hydrostatic inputs such as Centre of floatation about which rotational motions revolve for floating structures are extracted from this analysis and used as input data for the hydrodynamic analysis in ANSYS AQWA/HydroD.

2.2: Method

2.2.1: Numerical and Experimental Matrix

Table 4 shows matrix of operation developed to direct the order of investigations.

Two Methods of investigations, Numerical and Experimental, were conducted, although, the latter was designed to validate the numerical model. Each method of investigation was carried out in two stages for real response time history data to be captured: **(1) Tests with the Bare-hull FPSO model** moored at four positions; two at aft and the other two, forward and exposed simultaneously to four selected sea states namely,

International Journal of Advances in Engineering and Management (IJAEM)
Volume 6, Issue 09 Sep. 2024, pp: 321-339 www.ijaem.net ISSN: 2395-5252

180^o (Head Sea), 90^o (Beam Sea), 60^o and 30^o (Oblique seas). **(2) Tests under the same conditions as (1) above when the same arrangement of FPSO model is attached with Fins at selected positions on the Hull, such as** 0^o, 15^o and 30^o as shown in Figure 2.

The rationale was to quickly identify the effect of the attached fins on the motion responses evident from the Time History signatures by comparison after processing the time series response data in each case. It must be stated that both investigations were conducted under the same conditions with due regard to recommended guidelines by ITTC, (2015) for acceptable results.

Table 4: Developed Numerical and Experimental Matrix

Wave Directions/Fin angles for all Fin Sizes				
		WD30° (Oblique Sea)		
Stage 1		1	2	3
		FA0°	FA15°	FA30°
1	BH	1,1	1,2	1,3
No. of Runs		6	6	6
		WD60° (Oblique Sea)		
Stage 2		1	2	3
		FA0°	FA15°	FA30°
2	BH	2,1	2,2	2,3
No. of Runs		6	6	6
		WD90° (Beam Sea)		
Stage 3		1	2	3
		FA0°	FA15°	FA30°
3	BH	3.1	3,2	3,3
No. of Runs		6	6	6
		WD180°(Head Sea)		
Stage 4		1	2	3
		FA0°	FA15°	FA30°
4	BH	4.1	4,2	4.3
No. of Runs		6	6	6
TOTAL Runs	72	24	24	24

2.2.2 Numerical Model Analysis

Using the scaled principal particulars of the FPSO vessel, a model of the FPSO was produced and stability analysis ran in the MAXSURF ship hull modelling software to extract hydrostatic and stability parameters as inputs into the HydroD software for motion analysis. The body plan among the Model's lines plans as shown in Figure 5 generated from the MAXSURF enabled these parameters to be determined at the solution stage.

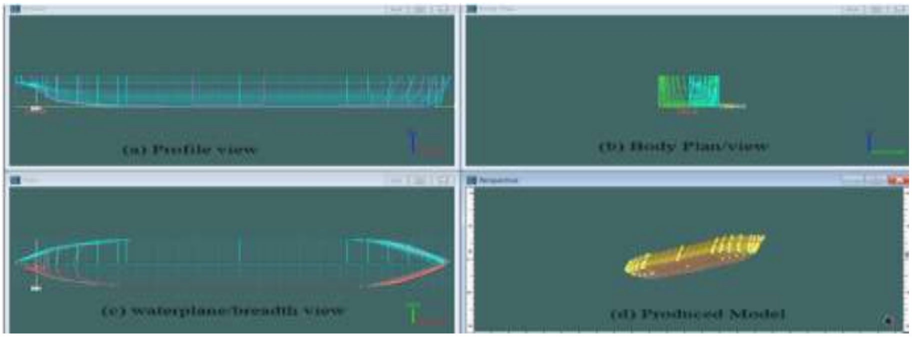

Figure 5: Lines Plans of FPSO Model Generated from MAXSURF

2.2.3 Theoretical Background for the Numerical analysis.

Equation (1) shows the theoretical model upon which the Numerical analysis is founded.

$$\overline{F}^{(2)} = -\int_{WL} \frac{1}{2}\rho g x \zeta_r^{(1)^2} . \overline{n}. dl + \overline{\alpha}^{(1)} x \left(M. \ddot{\overline{X}}_g^{(1)}\right) +- \iint_{S_0} \left\{ -\frac{1}{2}\rho \left|\overline{\nabla}\Phi^{(1)}\right|^2 - \rho\left(\Phi_{w_t}^{(2)} + \Phi_{d_t}^{(2)}\right) +- \rho \quad (1)$$

The theoretical foundation for the numerical analysis derives from the works of Johannes, (1980) who through a potential flow approximation provided measures to estimate the wave drift forces arising from difference frequencies of combining wave frequency pairs. According to his derivation,

International Journal of Advances in Engineering and Management (IJAEM)
Volume 6, Issue 09 Sep. 2024, pp: 321-339 www.ijaem.net ISSN: 2395-5252

the wave drift force also known as the horizontal component of the low and mean second order wave forces comprises of contributions from first order wave components. However, as also corroborated by Wichers, (2013), he held that the contributions of the second order potentials to the wave drift force, the fourth term in Equation (1), which may not be problematic in deep water is highly problematic in shallow waters because of the shallow water horizontal orbital velocity which shows strong presence at the sea bottom and so produces direct long wave excitation forces on moored structures in shallow waters. This is the problem under investigation.

2.2.4 Steps involved in Numerical analysis using ANSYS AQWA

ANSYS AQWA, a potential flow solver provides five basic solution routes for the delivery of effective results. These include (1) identification and insertion of hydrodynamic diffraction system and associated geometry. (2) identification and addition of AQWA specific parameters (3) and elements, (4) mesh geometry and generation and (5) analysis and post-processing.

The first stage involves building the model geometry for further processing in latter sections for solution. An effective model generation starts with the setting of units in conformity with defaults units within the simulation environment, identifying and specifying the type of analysis to be conducted. The second stage attempts to identify the general environment of the simulation software and conditions necessary to obtain accurate results. Selection of coordinate systems, density of water, water depth, point masses, structure parameters, etc., are all embedded in this stage. The program can compute the mass based upon the displacement of the vessel, or this can be defined directly in the details window.

The third stage, element identification and specification are very critical to the accuracy of the analysis as different engineering materials exhibit varieties of behaviors under prescribed constraints. Knowledge of the material properties of elements chosen for any simulation impacts positively on the simulation results as would a wrong choice of element produce a poor analysis outcome due to misrepresented element behavior different from the physical phenomena intended to be captured. In this analysis, a shell element was chosen for the modelling of the hull of the FPSO as it exhibits similar physical and structural properties of the material used in the construction of the hull.

The fourth stage, meshing operation discretizes a complex object into well-defined unit cells where the governing equation can be assigned so that the solver can easily simulate the physical behavior. Mesh generated for the solution stage enables accurate simulation of flow or other physical phenomena around the object.

Figure 6 (a), (b) and (c) respectively show meshed FPSO models with Fin attached at 0^o. 15^o and 30^o.

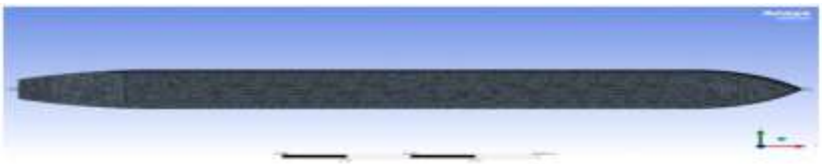

(a) Meshed Mystery FPSO Model with Fin attached at 0^O at Aft and Fore Peaks along the centreline of the FPSO Hull.

(b) Meshed Mystery FPSO Model with Fin attached at 15^O at Aft and Fore Peaks away from the centreline of the FPSO Hull

(c) Meshed Mystery FPSO Model with Fin attached at 30^O at Aft and Fore Peaks away from the centreline of the FPSO Hull

Figure 6: Meshed Mystery FPSO Models

International Journal of Advances in Engineering and Management (IJAEM)
Volume 6, Issue 09 Sep. 2024, pp: 321-339 www.ijaem.net ISSN: 2395-5252

2.2.5 Experimental Analysis

A 100year return wave period parameters shown in Table 1 were simulated in the NNPC/SPDC-JV Centre of Excellence (COE) Towing tank, Rivers State University, Port Harcourt against the prepared Wooden FPSO experimental model (see Figure 3) moored at four positions to the seabed and ballasted to the summer load-line, signifying fully loaded condition. **Refer to Figure 4.** The investigation water depth was 1.2m. It must be noted that the mooring lines, catenary in shape, only maintained the initial position for the freely floating model and did not produce any significant damping or restoration to the model. This was to ensure easy capturing of any amount of damping produced by the attached fins. Each run lasted for a minimum of 10 minutes for steady state responses to be captured before the next run until the final run as specified on Table 4. The point of attachment of fins (fin angle) were set at each run by a manual protractor scale positioned on the deck at the fore and aft peaks. The respective angles of wave attack on the model due to the incoming simulated wave was set by aligning the model to respective angles marked on an aluminum plate that was positioned directly under the model on the towing tank bottom.

III. RESULTS AND DISCUSSION

Figures 7, 8 & 9 comparative yaw time series response signatures for Bare hull and fin attached FPSO models for the investigated Sea conditions respectively for fin size 4.23mm, 8.46mm and 12.69mm. In all cases, the blue-coloured signatures are for the Bare hull response while the Orange-coloured signatures are for the Finned hull responses. It can be visualized the amount of yaw response damping created due to the attachment of the fin at each test case. However, the amount of damping and the frequency at which they occurred are shown respectively in Figures 10, 11 and 12. These figures show comparative spectral plot of Fourier transformed yaw time series responses for Bare hull and fin attached FPSO models for the investigated Sea conditions. It is observable from these figures that the maximum yaw response amplitude occurred at a very low frequency of 0.0781Hz for all cases while negligibly small response amplitudes occurred at relatively higher frequencies. The amount of damping effected by the fin in each case is shown in Figure 13.

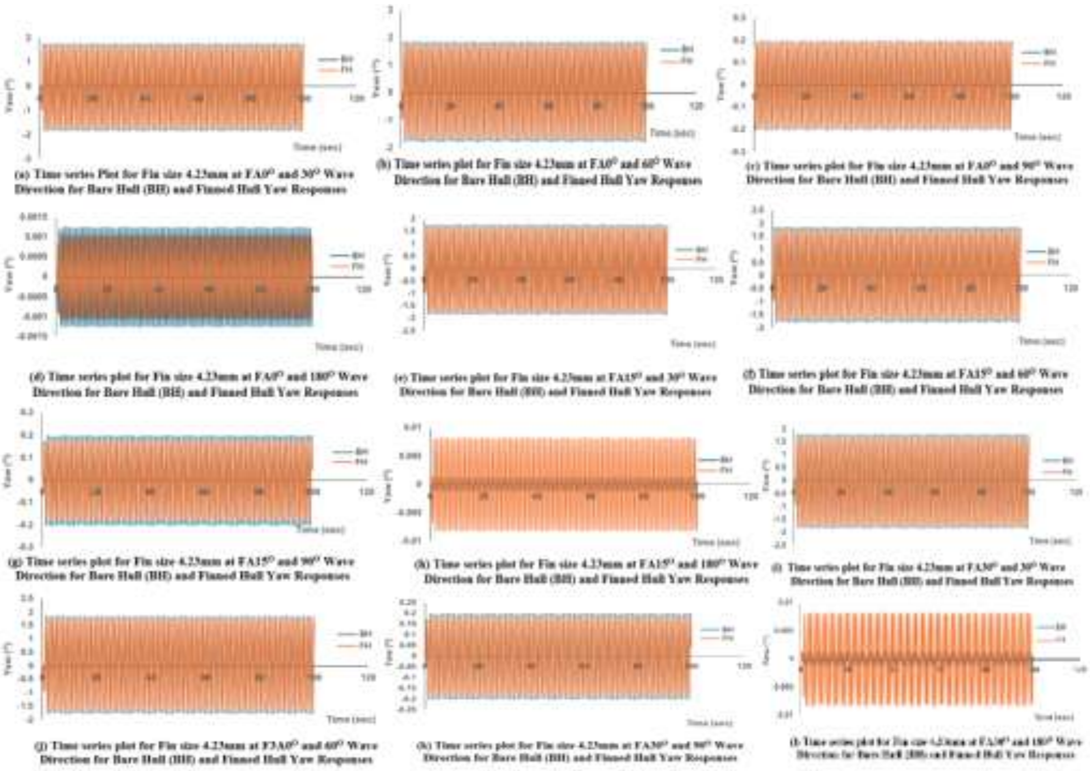

Figure 7: Yaw Response Amplitude Time series plot for fin size 4.23mm at all investigated wave directions and fin angles

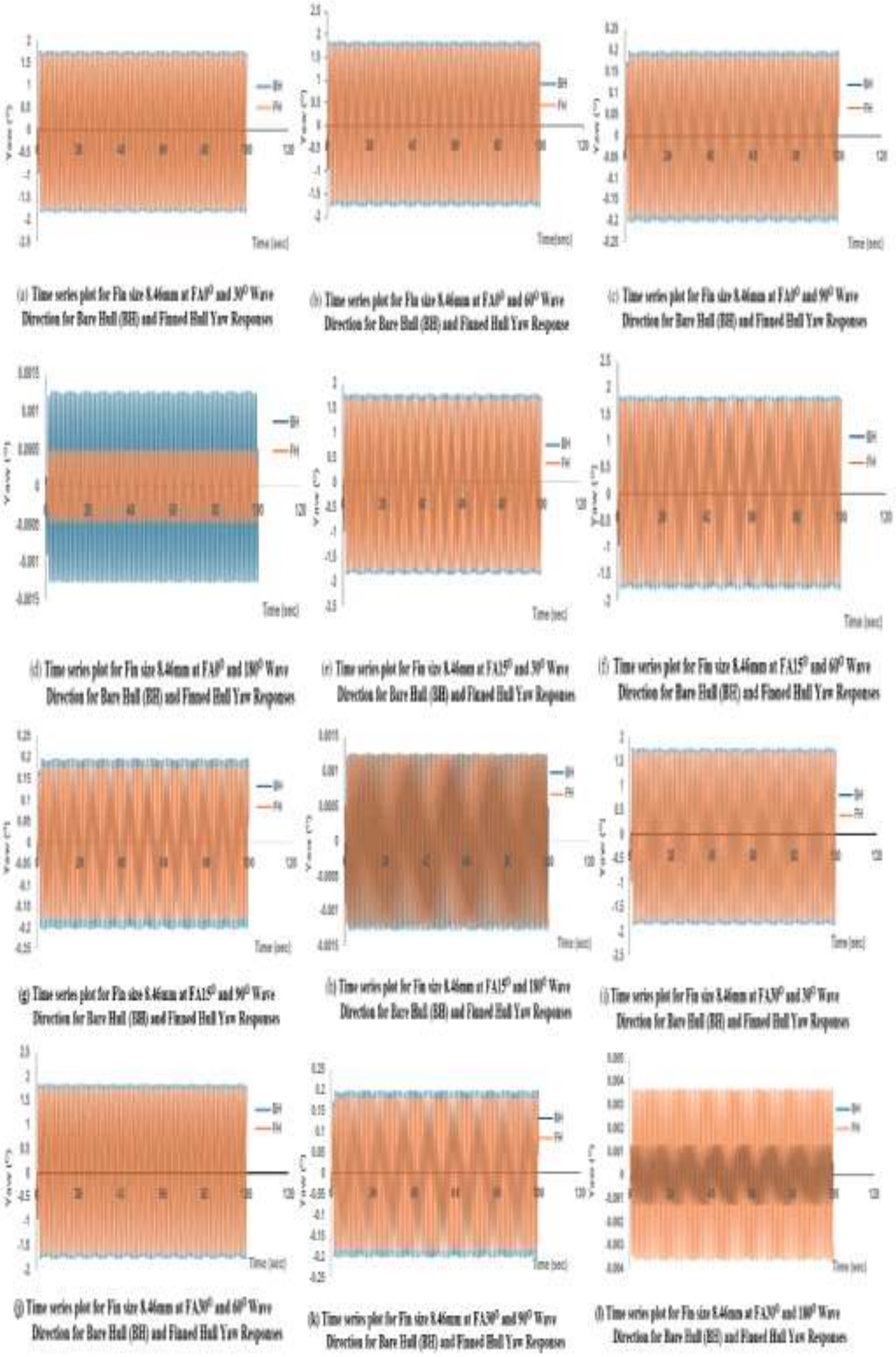

(a) Time series plot for Fin size 8.46mm at FA0° and 30° Wave Direction for Bare Hull (BH) and Finned Hull Yaw Responses

(b) Time series plot for Fin size 8.46mm at FA0° and 60° Wave Direction for Bare Hull (BH) and Finned Hull Yaw Response

(c) Time series plot for Fin size 8.46mm at FA0° and 90° Wave Direction for Bare Hull (BH) and Finned Hull Yaw Responses

(d) Time series plot for Fin size 8.46mm at FA0° and 180° Wave Direction for Bare Hull (BH) and Finned Hull Yaw Responses

(e) Time series plot for Fin size 8.46mm at FA15° and 30° Wave Direction for Bare Hull (BH) and Finned Hull Yaw Responses

(f) Time series plot for Fin size 8.46mm at FA15° and 60° Wave Direction for Bare Hull (BH) and Finned Hull Yaw Responses

(g) Time series plot for Fin size 8.46mm at FA15° and 90° Wave Direction for Bare Hull (BH) and Finned Hull Yaw Responses

(h) Time series plot for Fin size 8.46mm at FA15° and 180° Wave Direction for Bare Hull (BH) and Finned Hull Yaw Responses

(i) Time series plot for Fin size 8.46mm at FA30° and 30° Wave Direction for Bare Hull (BH) and Finned Hull Yaw Responses

(j) Time series plot for Fin size 8.46mm at FA30° and 60° Wave Direction for Bare Hull (BH) and Finned Hull Yaw Responses

(k) Time series plot for Fin size 8.46mm at FA30° and 90° Wave Direction for Bare Hull (BH) and Finned Hull Yaw Responses

(l) Time series plot for Fin size 8.46mm at FA30° and 180° Wave Direction for Bare Hull (BH) and Finned Hull Yaw Responses

Figure 8: Yaw Response Amplitude Time series plot for fin size 8.46mm at all investigated wave directions and fin angles

International Journal of Advances in Engineering and Management (IJAEM)
Volume 6, Issue 09 Sep. 2024, pp: 321-339 www.ijaem.net ISSN: 2395-5252

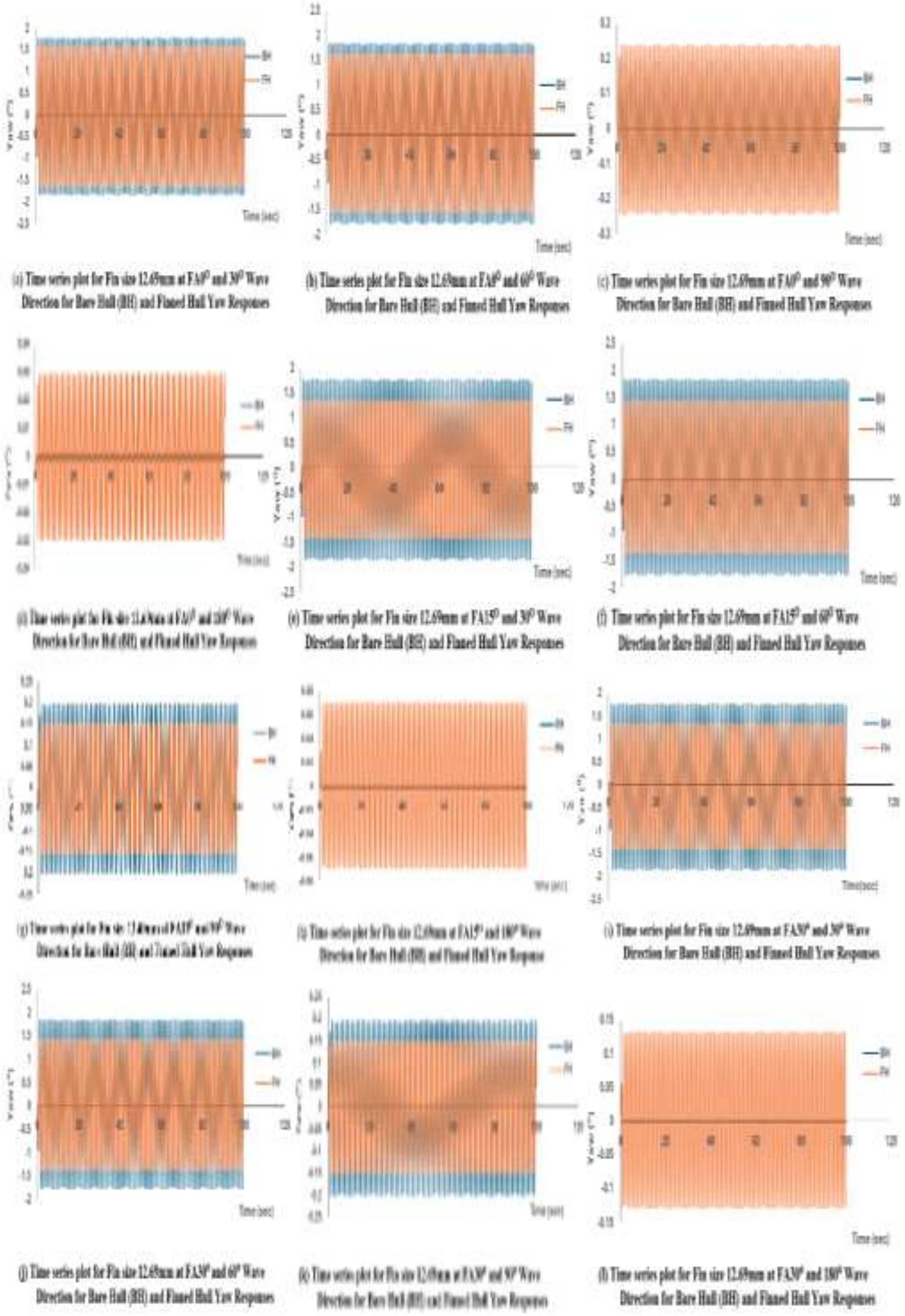

Figure 9: Yaw Response Amplitude Time series plot for fin size 8.46mm at all investigated wave directions and fin angles

International Journal of Advances in Engineering and Management (IJAEM)
Volume 6, Issue 09 Sep. 2024, pp: 321-339 www.ijaem.net ISSN: 2395-5252

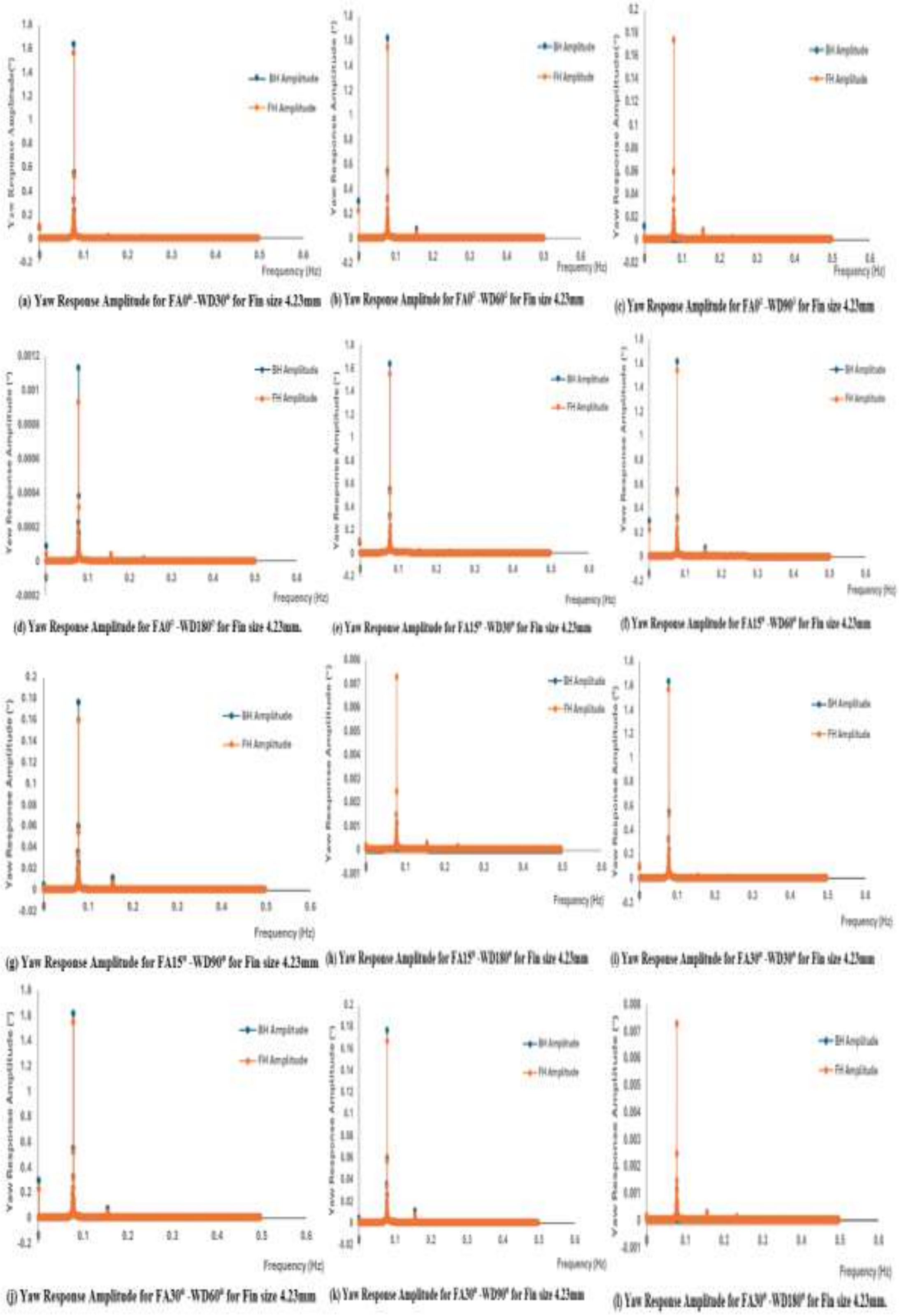

(a) Yaw Response Amplitude for FA0°-WD30° for Fin size 4.23mm (b) Yaw Response Amplitude for FA0°-WD60° for Fin size 4.23mm (c) Yaw Response Amplitude for FA0°-WD90° for Fin size 4.23mm

(d) Yaw Response Amplitude for FA0°-WD180° for Fin size 4.23mm. (e) Yaw Response Amplitude for FA15°-WD30° for Fin size 4.23mm (f) Yaw Response Amplitude for FA15°-WD60° for Fin size 4.23mm

(g) Yaw Response Amplitude for FA15°-WD90° for Fin size 4.23mm (h) Yaw Response Amplitude for FA15°-WD180° for Fin size 4.23mm (i) Yaw Response Amplitude for FA30°-WD30° for Fin size 4.23mm

(j) Yaw Response Amplitude for FA30°-WD60° for Fin size 4.23mm (k) Yaw Response Amplitude for FA30°-WD90° for Fin size 4.23mm (l) Yaw Response Amplitude for FA30°-WD180° for Fin size 4.23mm.

Figure 10: FFT Time series data for fin size 4.23mm for all investigation scenarios

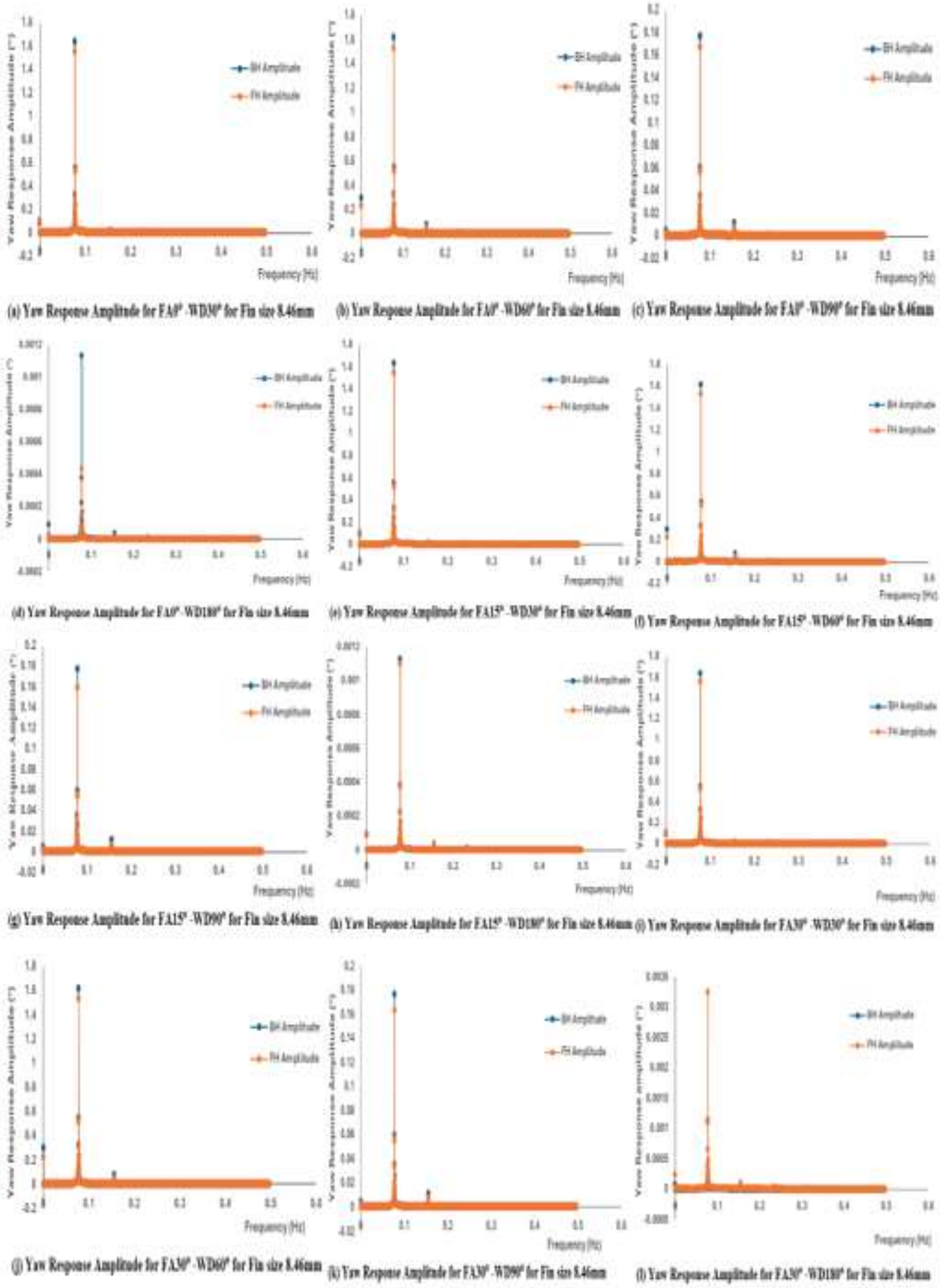

Figure 11: FFT Time series data for fin size 8.46mm for all investigation scenarios

International Journal of Advances in Engineering and Management (IJAEM)
Volume 6, Issue 09 Sep. 2024, pp: 321-339 www.ijaem.net ISSN: 2395-5252

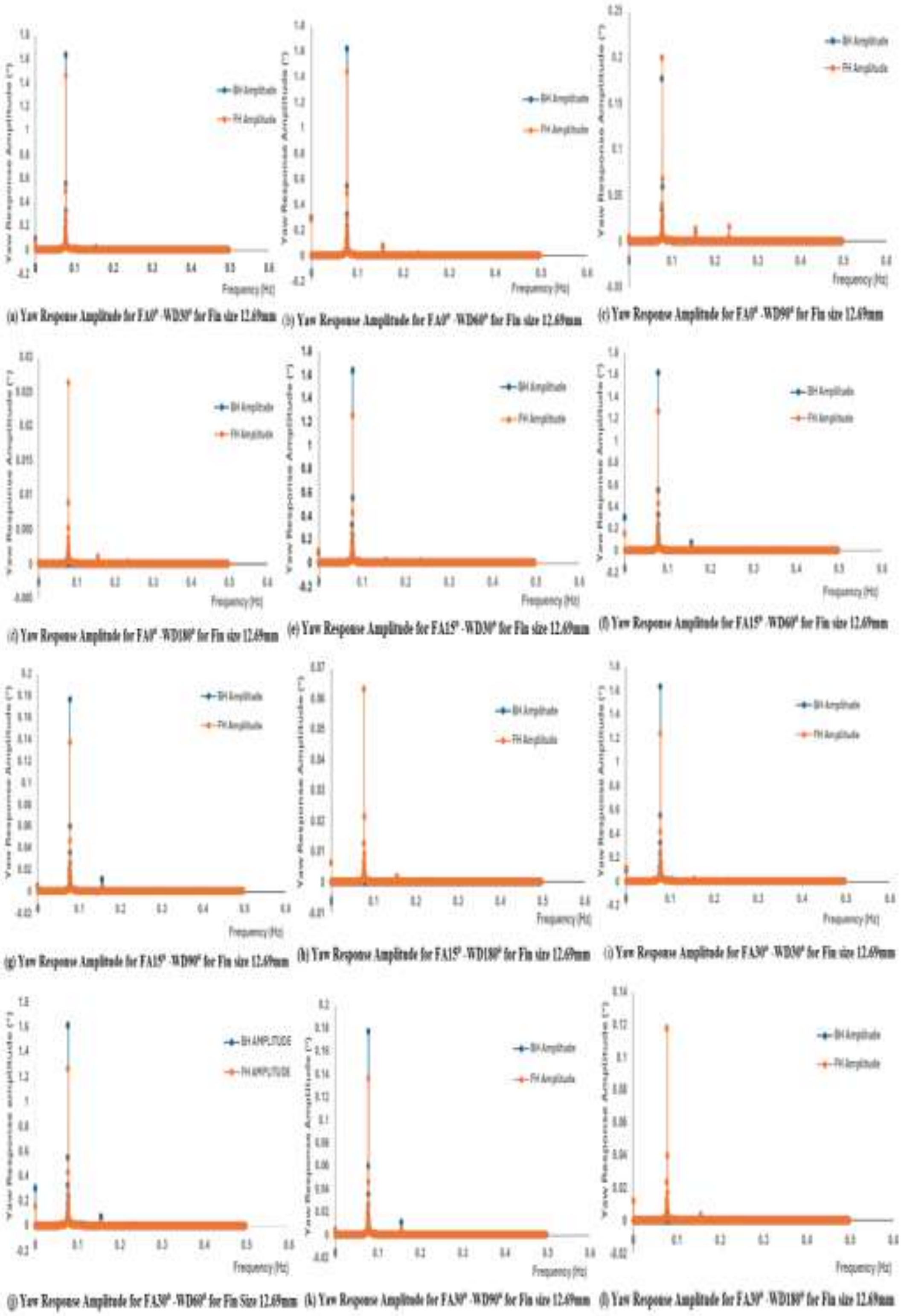

(a) Yaw Response Amplitude for FA0° -WD30° for Fin size 12.69mm (b) Yaw Response Amplitude for FA0° -WD60° for Fin size 12.69mm (c) Yaw Response Amplitude for FA0° -WD90° for Fin size 12.69mm

(d) Yaw Response Amplitude for FA0° -WD180° for Fin size 12.69mm (e) Yaw Response Amplitude for FA15° -WD30° for Fin size 12.69mm (f) Yaw Response Amplitude for FA15° -WD60° for Fin size 12.69mm

(g) Yaw Response Amplitude for FA15° -WD90° for Fin size 12.69mm (h) Yaw Response Amplitude for FA15° -WD180° for Fin size 12.69mm (i) Yaw Response Amplitude for FA30° -WD30° for Fin size 12.69mm

(j) Yaw Response Amplitude for FA30° -WD60° for Fin Size 12.69mm (k) Yaw Response Amplitude for FA30° -WD90° for Fin size 12.69mm (l) Yaw Response Amplitude for FA30° -WD180° for Fin size 12.69mm

Figure 12: FFT Time series data for fin size 12.69mm for all investigation scenarios

International Journal of Advances in Engineering and Management (IJAEM)
Volume 6, Issue 09 Sep. 2024, pp: 321-339 www.ijaem.net ISSN: 2395-5252

Figure 13 presents summary Bar plots of percentage reduction in yaw response amplitudes for the investigated cases via a statistical analysis of the Fast Fourier Transformed yaw time series data obtained from the numerical simulation. These plots enable numerical quantification of the amount of reduction in yaw response amplitude achieved by the attachment of fins to the FPSO hull.

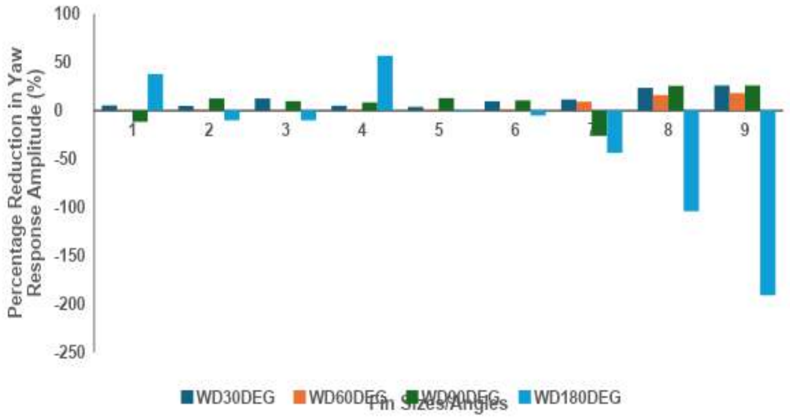

Figure 13: Summary Comparative plot of % Reductions in Yaw Response Amplitudes for all Wave Directions and Fin angles

For all the 72 investigation points, 24 each for Fin size, shown in Figures 13, Fin size 8.46mm produced the highest percentage Positive reduction in Yaw response (10 Positive cases), followed by Fin size 4.23mm (9 Positive cases) and the least being Fin size 12.69mm (8 Positive cases). These are respectively, 83.33%, 75%% and 66.67%. Also, the order of decreasing percentage Negative impact on yaw response amplitude reduction are 33.33% for Fin size 12.69mm (4 Negative cases), 25% for Fin size 4.23mm (3 Negative cases) and 16.67% for Fin size 8.46mm (2 Negative cases).

In terms of the number of investigated cases for each Fin size for which some percentage reductions in yaw response amplitude are positive while others are negative, we can therefore conclude that Fin Size 8.46mm produced the highest Positive percentage reductions in yaw response amplitude while the least is fin size 12.69mm. Taking the numerical average for each Fin size, of all the Positive percentage reductions in yaw response amplitude however, shows that Fin size 12.69mm produced the highest percentage reduction in yaw response amplitude followed by Fin size 8.46mm and the least being Fin size 4.23mm. The percentage average values respectively are 18.75%, 10.55% and 8.89%.

In terms of Positive percentage reduction in value in all cases, it was observed that the Fin size 12.69mm performed better than all other Fin sizes. These two analyses screen out Fin size 4.23mm in terms of the best Fin size of choice for yaw response amplitude reduction in the investigated scenario; the two contending Fin sizes being Fin size 12.69mm and 8.46mm.

Now from Figure 13, it could also be observed that the Single highest percentage reduction in yaw response amplitude (56.7%) occurred at the head sea condition with fin size 8.46mm and fin angle 0^o while for Fin size 12.69mm, this single highest percentage reduction (25.97%) occurred at Oblique Sea direction 30^o and Fin Angle 30^o. This result could make Fin Size 8.46mm the Fin Size of choice as it also produced the least Negative percentage reduction in yaw response amplitude (16.16%) relative to the contending Fin Size 12.69mm that has highest negative impact on yaw response amplitude damping (33.33%).

However, since the core of this investigation is to conclude on the Fin Size and Angle of attachment at given Wave Direction that presented the best all positive yaw response amplitude damping for effective operation of the FPSO, Fin Size 8.46mm becomes the preferred Fin Size. It produced all-positive reduction in yaw response amplitudes across all Wave Directions with an average percentage reduction of 17.8%. In Figure 13, the highest percentage reduction of 56.69% was achieved at the Head Sea condition followed by 8.44% reduction at the Beam Sea condition and the least percentage reductions (5.05% at 30^o and 1.04 at 60^o) at Oblique Sea conditions.

Increasing Fin Size from 4.23mm to 8.46mm for the Head Sea condition produced a

International Journal of Advances in Engineering and Management (IJAEM)
Volume 6, Issue 09 Sep. 2024, pp: 321-339 www.ijaem.net ISSN: 2395-5252

marked 49.93% increase in percentage reduction in yaw response amplitude whereas, a further increase in Fin Size from 8.46mm to 12.69mm at the Head Sea condition saw all the gains in previous increase deteriorated to a negative value (-4369.88%). At the Beam Sea condition and at Fin Angle 0^o, only Fin Size 8.46mm produced a positive percentage reduction in yaw response amplitude whereas, percentage reductions produced by Fin Sizes 4.23mm and 12.69mm are all negatives. Again, across Fin Angles, only Fin Size 8.46mm Produced all Positive percentage reduction with an average of 10.6% for the Beam Sea Condition. This makes Fin Size 8.46mm at the Head and Beam Sea conditions the best option.

For the Oblique Sea conditions (30^o and 60^o), all Fin Sizes at the considered points of attachment to the hull appeared to be doing well as all percentage reductions are positive with the highest (25.97%) occurring at Fin Angle 30^o and Wave Direction 30^o for Fin Size 12.69mm. The average percentage reduction across all Fin Sizes for the best Oblique Sea condition (30^o) are respectively 7.6%, 6.2% and 20.3% for Fins Sizes 4.23mm, 8.46mm and 12.69mm. Therefore, for moored floating structures like FPSO that should be positioned at a given heading based on a sound knowledge of the Sea directions for operational safety, it is can be concluded that positioning the investigated Finned Hull FPSO in the Oblique direction to the predominant direction of the Seas, for all Fin Sizes, will also positively dampen yaw response amplitude; the best performance being the 30^o Oblique Sea condition with Fin Size 12.69mm.

Overall, however, it is concluded that, fin size 8.46mm at 0^o point of attachment despite having lower average percentage reduction in yaw motion response amplitude relative to fin size 12.69mm presented the best operational safety net for the FPSO in all tested sea states. This is true as it is more practical, as design requires, for moored FPSOs to face impact from site-specific sea conditions, whether in the pure or interacting forms, for operational survivability and not for impact from a single sea state.

3.1 Validation of Numerical Model

Results from experiment to validate the accuracy of the numerical models for Oblique wave directions 30^0 and 60^0 are presented in Figures 14 and 15.

The Fast Fourier Transformed time series plots in Figure 14 showed the same trend for both methods of investigation, although with the numerical responses slightly peaking at higher frequency of 0.0781 Hz than the experimental responses which peaks at 0.0717 Hz. The low frequency area had the highest peaks for all scenarios.

Figure 15 shows comparative Bar plots incorporating Error bars of statistically analyzed Fast Fourier Transformed time series data for both numerical and experimental investigations. Obviously, the trends for both the numerical and experimental investigation results are similar as seen in Figure 15. An average percentage yaw response amplitude reduction for numerical and experimental results at WD30^0 and WD60^o were observed to be 20.33% against 21.23%, and 14.51% against 16.96% respectively. This showed semblance of both results with negligible percentage differences of 0.9% for wave direction 30^o and 2.45% for wave direction 60^o**.** The differences between compared experimental and numerical results as depicted in Figure 15 are respectively, 1. 808%, 0.032%, 0.862%, 4.802%, 1.875% and, 0.581% for FA0^o-WD30^o, FA15^o -WD30^o, FA30^o -WD30^o, FA0^o -WD60^o, FA15^o -WD60^o and, FA30^o -WD60^o. Clearly therefore, FA15^o -WD30^o with the least difference of 0.032% between experimental and numerical results presented the best basis for comparison while the worst case was FA0^o -WD60^o with highest difference of 4.802%. The error bars also confirmed this position as overlap of the error bars between measured and predicted datasets in each case indicated statistical indifference between these datasets showing how close these datasets compared. This overlap is more with FA15^o -WD30^o and non-existent for FA0^o -WD60^o indicating that it was only at FA0^o -WD60^o among all the investigated cases where there existed statistical difference between the measured and predicted datasets.

Overall, wave direction 30^o with the least average percentage reduction in yaw response amplitude of 0.9% against 2.42% for wave direction 60^o presented the best results based on the compared percentage reduction in yaw response amplitude achieved in the validation case

To validate the numerical model, Root-Mean-Square-Error analysis was performed between predicted (simulation) and measured (Experimental) datasets. Summary results from this analysis as shown in Table 5 demonstrated very close relationship between these two datasets in all investigated scenarios for the validation. This confirmed how close the numerical procedure represented the physical phenomenon investigated.

International Journal of Advances in Engineering and Management (IJAEM)
Volume 6, Issue 09 Sep. 2024, pp: 321-339 www.ijaem.net ISSN: 2395-5252

A root-mean-square-error of approximately 0.1 across all investigated cases amounts to about 90% accuracy of the numerical model in representing the physical phenomena thus, it is concluded that the developed model can appropriately solve the problem investigated within an error margin of 10%. Since numerical and experimental investigation procedures were similar, it suffices to conclude that within the same root-mean-square-error of 10%, the same results will obtain between predicted and experimental datasets for fin sizes 4.23mm and 8.46mm.

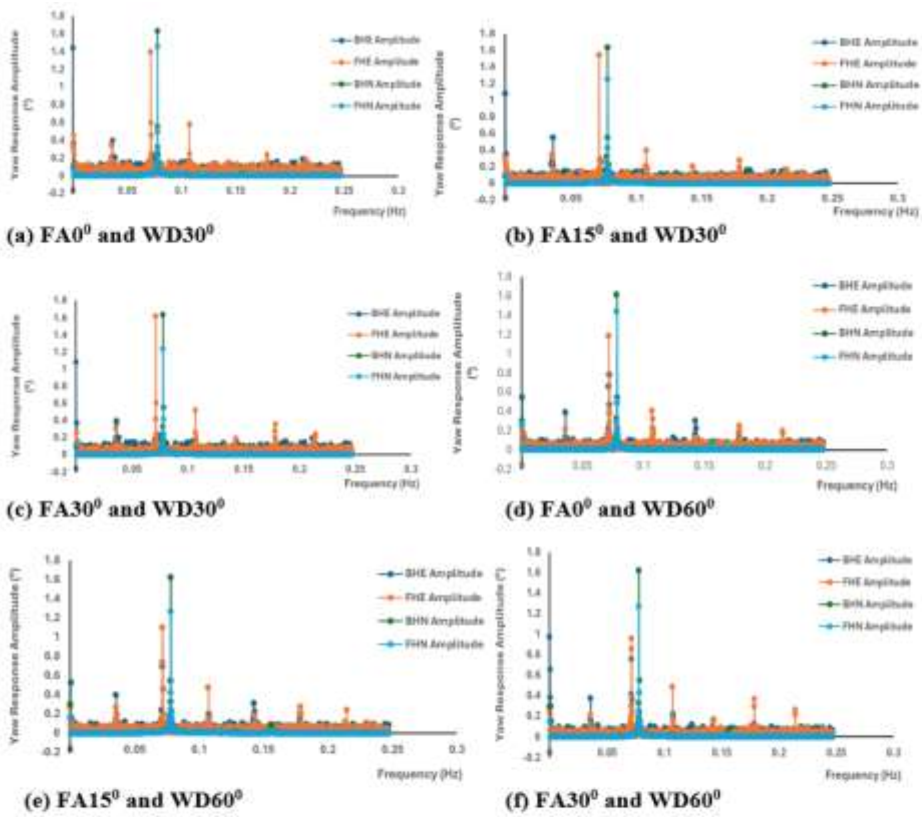

Figure 14: Validation Plot comparing Experimental and Numerical FFT time series data for Oblique Sea conditions (30^0 and 60^0) for all fin angles considered

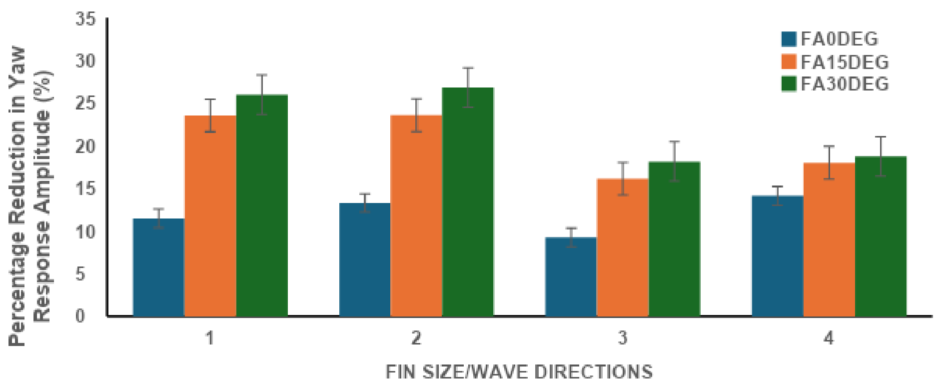

Figure 15: Validation Component Bar Plots comparing Numerical and Experimental Percentage Reduction in Yaw Response Amplitude

International Journal of Advances in Engineering and Management (IJAEM)
Volume 6, Issue 09 Sep. 2024, pp: 321-339 www.ijaem.net ISSN: 2395-5252

Table 5: Summary Validation Root-Mean-Square-Error Analysis Results

	FA0^o-WD30^o	FA15^o-WD30^o	FA30^o-WD30^o	FA0^o-WD60^o	FA15^o-WD60^o	FA30^o-WD60^o
BH (EXP/NUM)	0.0857378	0.083273612	0.083315604	0.08364372	0.083643717	0.08501937
FH (EXP/NUM)	0.0906296	0.08194333	0.08484312	0.0781692	0.076550593	0.07441389

IV. CONCLUSION

The study sets out to identify, among selected fin sizes, the best Fin Size, point of attachment on the FPSO hull and the best wave direction suitable to dampen problematic shallow water-induced large yaw response amplitude arising from wave drift forces which is critical to safe operation and improved station keeping of the FPSO vessel. Three rectangular Fin Sizes of widths 4.23mm and aspect ratio of 0.0313, 8.46mm and aspect ratio of 0.0627 and 12.69mm and aspect ratio of 0.094 at three selected angles of attachments to the FPSO hull such as 0^o, 15^o and 30^o were modelled in Ansys Aqwa and simulated against 100 year return period wave conditions characteristic of the Gulf of Guinea in three Wave Directions, namely; Head, Beam and Oblique Seas which are critical to yaw motion response. By adopting numerical solution approach and validation through experimentation, investigations were performed for two scenarios of the FPSO namely, the Finned Hull FPSO and the Bare Hull FPSO which stands as the control. From results obtained, it can summarily be stated that:

- For the considered Fin angles and sea conditions, the Head Sea condition presented the highest percentage reduction in yaw motion response amplitude, as much as 37.81% for Fin size 4.23mm attached at 0^0 to the hull of the FPSO. However, for all the considered Fin angles for Fin size 4.23mm, the Oblique Sea direction (30^o) presented the best all-positive percentage reductions in yaw motion response amplitude with an average of 7.6%.
- The Head Sea condition among all considered sea directions presented the highest percentage reduction in yaw motion response amplitude, as much as 56.69 % for Fin size 8.46mm attached at zero degree to the hull of the FPSO. However, for all the considered Fin angles for Fin size 8.46mm, the Beam Sea direction (90$^{o)}$ presented the best all-positive percentage reductions in yaw motion response amplitude with an average of 10.6%.
- The Oblique Sea condition (30^o) among all considered sea directions presented the highest percentage reduction in yaw motion response amplitude, as high as 25.97% for Fin size 12.69mm attached at 30^o to the hull of the FPSO. Strikingly, for all the considered Fin angles for Fin size 12.69mm, the 30^o Oblique Sea condition again, produced the best all-positive percentage reductions in yaw motion response amplitude with an average of 20.3%.
- Overall, Fin size 8.46mm at 0^o point of attachment presented the best operational safety net for the FPSO in all Sea States considered for yaw response amplitude damping as it is more practical for moored FPSO to be impacted upon by all site-specific Sea conditions while in operation rather than a single sea condition (oblique sea 30^o) for which fin size 12.69mm is better. This is true as percentage yaw response amplitude dampening across all Wave directions are positive for Fin size 8.46mm attached at 0^o on the Hull of the FPSO vessel. The lower average percentage reduction across wave directions of 17.8% relative to a higher average percentage reduction (20.3%) for Fin size 12.69mm at oblique sea 30^o notwithstanding. Thus, the optimum fin size is 8.46mm among the selected fin sizes for sensitivity studies.

It is noted interestingly that the results obtained in this study compared with the works of Rajesh et al., 2016 which achieved between 58% to 80% reduction in pitch motion for a speed range of 5-25knots by the application of deeply submerged fins at the bow region of a container ship thus, guaranteeing crew safety and a savings in money. Of course, a higher reduction in motion response is expected by the application of fins for vessels with forward speed as fin is more active in that regime making use of its high lift property with accompanying large moment to effectively dampen vessel vertical motion. Again, it is worth mentioning that the success achieved in this study has given impetus to the extensive application of the rules governing selection of bilge keels, positioning and orientation to fins as posited by (Rajesh et al., 2016; McTaggart, 2004 and Wendi et al., 2019). Recommendations from these works guided the selection of fin parameters for this study even though, some deviations were considered such as the fin profile and orientation which made this work unique.

ACKNOWLEDGEMENTS

The authors are grateful to the management of NNPC/SPDC-JV COE, River State University, Port Harcourt for granting access to her facility without which validation of this work would have been difficult. Due regards are also to the technical staff of the Laboratory whose inputs are invaluable.

NOMENCLATURE

Symbols	Description and Units	
	Fluid density	Kg/m^3
	Velocity potential	s^{-1}
	Gradient function	m^{-1}
	Oscillatory first order angular motion vector	rad/s
	Second order motion vector of the Centre of gravity of the body	m/s
	First order motion	m/s
	Gravity constant	m/s^2
	A surface element	m
	Elemental length	m
	Inertia mass	Kg
	Integral over the waterline	
	Normal vector of a point on the surface of the structure	
	Double integral over the surface element	
	Time dependent second order diffraction wave potential	s^{-1}
	Time dependent undisturbed incoming second order wave potential (Froude-Krylov term)	s-1
	First order wave potential	s^{-1}
	Relative first order wave elevation	m
	Total second order force	N
	Percentage	%
Acronyms	**Meaning**	
	Numerical	
	Experimental	
	Bare Hull Experimental	
	Bare Hull Numerical	
	Finned Hull Experimental	
	Finned Hull Numerical	
COE	Centre of Excellence	
	Fast Fourier Transform	
	Bare Hull	
	Finned Hull	
	Fin Angle	$(^0)$
	Wave Direction	$(^0)$
	Degrees	$(^0)$

REFERENCES

[1]. Ekwere, D. E., Ibiba, D. E., Dick, I. F., & Morrison, I. (2021). Free span analysis of an offshore pipeline in the gulf of Guinea. American Journal of Engineering, 10(05), 49-64.

[2]. Greco, M., Lugin, C., & Faltinsen, O. M. (2015). Influence of motion coupling and nonlinear effects on parametric roll for a FPSO platform. Philosophical transaction, 1-18.

[3]. IMCA M 121, (2016). DP Position loss risks in shallow water. International Marine Contractors Association, 1-24. www.imca-int.com/marine.

[4]. ITTC. (2005). Recommended Procedures and Guidelines, Testing and extrapolation Methods,Loads and Responses, Ocean Engineering Floating Offshore Platform Experiments.International Towing Tank Committee, 1-12.www.ittc.info

[5]. Jaime, T. L., & Longbin, T. (2017). Experimental study on the hydrodynamic behaviour of an FPSO in a deep water Region of the Gulf of Mexico. Elsevier, 1-82.

[6]. Johannes, A. P. (1980). Low frequency second order wave excitation forces on

[7]. Li, X., Yang, J., & Xiao, L. (2003). Motion analysis on a large FPSO in shallow water. Proceedings of the 13th International Offshore and Polar Engineering Conference, (235-239).

[8]. Lingzhi, X., Haining, L., Jianmin, Y., & Wenhua, Z. (2015). Motion Responses of a Moored Barge in Shallow Water.

[9]. McTaggart, K. (2004). Appendages and viscous forces for ship motion in waves. Canada: Defence Research and Development.

[10]. Molin, B., & Fauveau, V. (1984). Effect of Wave-directionality on Second-order Loads Induced by the Set-down. Applied Ocean Research, 6(2), 66-72.

[11]. Naciri, M., Buchner, B., Bunnik, T., Huijsmans, R., & Andrews, J. (2004). Low-frequency motions of LNG carriers moored in shallow water. ASME 2004 23rd Innternational Conference on Offshore Mechanics and Arctic Engineering, 3, 995-1006. Canada.

[12]. Pinkster, J. (2009). Wave drift forces in directional seas in shallow water. ASME 2009 28th Conference on Ocean, Offshore and Arctic Engineering, (831-842).

[13]. Rajesh Reguram, B., Surendran, S., & Seung, K. L. (2016). Application of fin system to reduce pitch motion. International Journal of Naval Architecture and Ocean Engineering, 409-421.

[14]. Sanchez-Mondragon, J., Vazquez-Hernandez, O. A., Cho, S., & Sung, H. (2018). Yaw motion analysis of a Turret mooring system under wave drift forces. Applied Ocean Research.

[15]. Smith, T., & Thomas III, W. (1990). A Survey of Ship Motion Reduction Devices. David Taylor Research Centre, Ship Hydromechanics. Bethesda Maryland: United States Navy.

[16]. Wendi, L., Yigit, K. D., Eko, B. D., Setyo, N., Tahsin, T., Rafet, E. K., . . . Atilla, I. (2019). Bilge Keel Design for the traditional fishing boats of Indpnesia's East Java. International Journal of Naval Architecture and Ocean Engineering, 11, 380-395.

[17]. Wichers, I. J. (2013). Guide to single point Moorings (1st ed.). WMoorings, Inc. 1-455.

[18]. Wim, v., & Ivo, W. (2008). Time-domain calculations of moored ship motions in non-linear waves. Coastal Engineering, 55(5), 409-422.

[19]. Yan, S., Ma, Q., Lu, J., & Chen, S. (2010). Fully non-linear analysis on responses of a moored FPSO to waves in shallow water. Proceedings of ISOE2010. Beijing.

[20]. Yang, J., Xiao, L., & Peng, T. (2002). Experimental research on motion performance of larde FPSO in shallow water. Proceedings of the third New S-Tech Conference. Kobe, Japan.

[21]. Yanlin, W., Zheliang, F., Du, Y., Shanshan, S., Guoxun, Z., & Qianjin, Y. (2015). Integrity Assessment of Soft Yoke Moored FPSO for the Hinge Point Problems. The Twenty-fifth International Ocean Polar Engineering Conference. International Society of Offshore and Polar Engineers (ISOPE), Kona, Hawaii, USA.